Journal of Magnetic Resonance **138,** 155–159 (1999)
Article ID jmre.1998.1675, available online at http://www.idealibrary.com on IDEAL®

COMMUNICATIONS

Gas Flow MRI Using Circulating Laser-Polarized ^{129}Xe

E. Brunner, M. Haake,* L. Kaiser,[1] A. Pines, and J. A. Reimer*

*Materials Sciences Division, Lawrence Berkeley National Laboratory, and *Departments of Chemistry and Chemical Engineering, University of California, Berkeley, California 94720*

Received July 6, 1998; revised November 18, 1998

We describe an experimental approach that combines multidimensional NMR experiments with a steadily renewed source of laser-polarized ^{129}Xe. Using a continuous flow system to circulate the gas mixture, gas phase NMR signals of laser-polarized ^{129}Xe can be observed with an enhancement of three to four orders of magnitude compared to the equilibrium ^{129}Xe NMR signal. Due to the fact that the gas flow recovers the nonequilibrium ^{129}Xe nuclear spin polarization in 0.2 to 4 s, signal accumulation on the time scale of seconds is feasible, allowing previously inaccessible phase cycling and signal manipulation. Several possible applications of MRI of laser-polarized ^{129}Xe under continuous flow conditions are presented here. The spin density images of capillary tubes demonstrate the feasibility of imaging under continuous flow. Dynamic displacement profiles, measured by a pulsed gradient spin echo experiment, show entry flow properties of the gas passing through a constriction under laminar flow conditions. Further, dynamic displacement profiles of ^{129}Xe, flowing through polyurethane foams with different densities and pore sizes, are presented.

Key Words: **laser-polarized ^{129}Xe; MRI; gas flow imaging; continuous flow.**

INTRODUCTION

Magnetic resonance imaging (MRI) is a well-established analytical technique in medicine and materials sciences (*1*). A serious limitation in MRI of gases is the low density in the gas phase compared to condensed phases (e.g., water) and the relatively low equilibrium nuclear spin polarization. One way to achieve a reasonable signal-to-noise ratio, without time-consuming signal averaging, is to use fluorine-rich gases (C_2F_6) at elevated pressure (~0.7 MPa) (*2*). Increasing interest has developed in the enhancement of sensitivity and contrast in MRI using laser-polarized noble gas nuclei such as ^{3}He or ^{129}Xe (*3–6*). The gas circulation system described in (*7*) delivers a continuous flow of laser-polarized ^{129}Xe. The nonequilibrium ^{129}Xe nuclear spin polarization can exhibit spatial variations due to longitudinal relaxation. It is, however, time-independent under laminar flow conditions in steady state. The steady-state nonequilibrium ^{129}Xe nuclear spin polarization attainable in this system recovers the starting conditions for each acquisition in a short time (0.2–4 s), depending on the sample density and differential pressure applied. Therefore experiments are no longer limited in time by longitudinal relaxation. Pulse sequences requiring a steadily renewed nuclear spin polarization can now be applied without any restriction; phase cycling and signal averaging are feasible.

In the following we describe how to combine the method of circulating laser-polarized ^{129}Xe with MRI technology. Fourier images of a phantom sample and dynamic displacement profiles of gas flowing through a constriction and through open cell polyurethane (PU) foams of different densities and pore sizes are presented.

EXPERIMENTAL

The gas circulation system (*7*) consists mainly of (i) a homebuilt apparatus similar to the one designed by Driehuys *et al.* (*8*), providing a continuously flowing gas stream carrying the laser-polarized ^{129}Xe gas, and (ii) a homebuilt probe (*9*) with a solenoid coil (flat copper, 2 cm long, 1 cm wide). The probe is equipped with a commercial, air-cooled gradient system (Bruker) with a horizontal bore. It produces a maximum gradient of 0.6 T/m corresponding to ca. 7 kHz/mm for ^{129}Xe. A Chemagnetics spectrometer (Infinity) and a super wide-bore (115 mm) Nalorac superconducting magnet with a B_0 of 4.2 T in z direction are used. The gradient unit is powered by three Techron 7550 amplifiers. The gas mixture, containing 40 kPa of natural abundance xenon and 27 kPa of N_2, was pressurized with ^{4}He (up to 1 MPa). It is circulated through the system using a pressure- and vacuum-resistant pump (Brey GK-M07), producing a maximum flow rate of ca. 30 ml/min at a differential pressure of up to 15 kPa through 3.2-mm copper tubing. The Rb atoms are optically pumped in the fringe field of the superconducting magnet at the wavelength of the Rb D_1 transition (~795 nm) with circularly polarized light from a liquid-

[1] To whom correspondence should be addressed. Fax: 510 486 5744. E-mail: lana@dirac.cchem.berkeley.edu.

1090-7807/99 $30.00

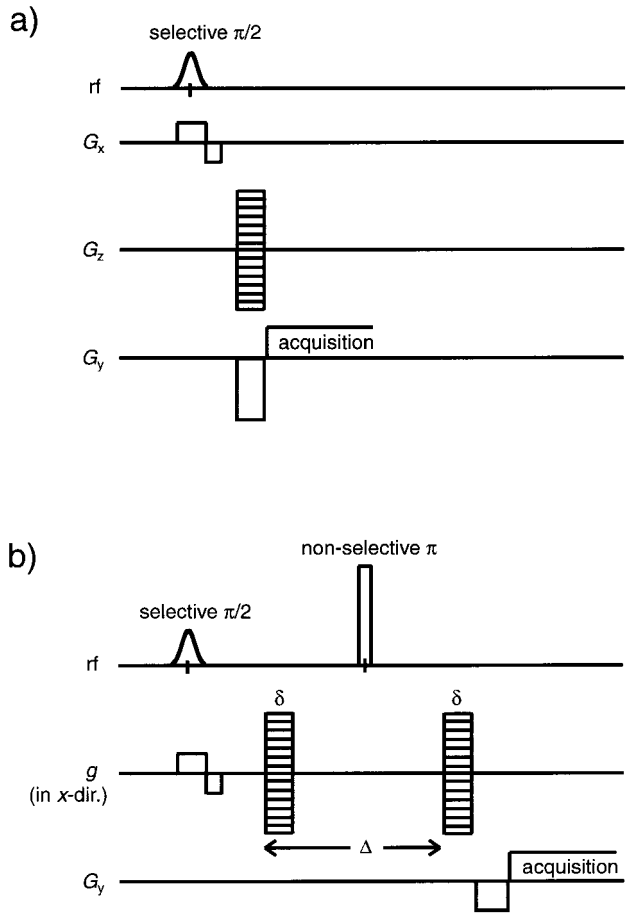

FIG. 1. (a) Pulse sequence used for Fourier imaging. (b) Modified PGSE sequence for combined *k*-space and *q*-space imaging (dynamic NMR microscopy) to produce velocity profiles.

cooled IR laser diode array (Optopower Corp., Model OPC-A150-795-RPCZ), delivering about 90 W light power at wavelengths of 795 ±1 nm. Passing through the optical pumping cell, the xenon gas is polarized "on the fly" up to 3%, which is more than three orders of magnitude higher than the thermal polarization of ^{129}Xe. The gas mixture is cooled in a condenser to remove Rb before entering the detection zone inside the superconducting magnet. Finally, the mixture reenters the gas circulation pump to start a new cycle.

FOURIER IMAGING RESULTS

Figure 1a shows the two-dimensional (2D) Fourier imaging pulse sequence also denoted as spin warp sequence (*1*) that was used to detect the *yz* image of a phantom sample displayed in Fig. 2 (the gas flows in *x* direction). An inversion recovery experiment proved that the xenon in the detection zone was completely exchanged after 1 s. A repetition time of 1.5 s was therefore chosen during the accumulation of 16 scans (*10*) resulting in a *S*/*N* ratio of 20. The data were acquired as a 256 × 128 matrix, using 128 phase-encoding steps and a read gradient of 0.6 T/m. After 2D Fourier transformation, a magnitude calculation was carried out. The pixel size is 110 × 340 μm for the raw data shown in Fig. 2a. The phantom sample used in the experiment was a glass tube (7 mm id) containing one sealed and eight open-ended capillaries (1.3 mm od), parallel to the gas flow direction (x), each having a wall thickness of ca. 200 μm. These capillaries are visible as dark circles in the original density image. The recomputed image is shown in Fig. 2b after zero-filling the data matrix to 512 × 512 data points and subsequent interpolation using cubic splines. The capillary that was flame-sealed on both ends (white dotted circle) contains no xenon and remains dark.

Imaging resolution is affected and limited by molecular diffusion. Our setup uses pressure up to 1 MPa, and the image presented here was taken at 0.4 MPa. For gas mixtures, the diffusion coefficient, D, can be calculated using the formulae given in (*11*), which we calculated to be 0.1–0.2 cm^2/s. The maximum imaging resolution is limited to about $2 \times 1_g$, where 1_g is given by $1_g = (D/(\gamma G))^{1/3}$ (*12*). This gives a maximum resolution of $2 \times 1_g$ (120–150 μm for our experiment). If necessary, the parameter $2 \times 1_g$ limiting the resolution can be further reduced by increasing the pressure, since D is inversely proportional to the pressure. The maximum pressure, which can be used in our apparatus safely, amounts to ca. 1 MPa (corresponding to 90–110 μm for $2 \times 1_g$).

In addition, images taken in flow direction would be affected by the displacement of the gas mixture during data acquisition time (~1 ms). Within this time the slice moves 50 to 70 μm at an average velocity of 5 to 7 cm/s, assuming laminar flow. Another source of distortion is due to relaxation effects of the xenon spins during surface contact with the sample. In our circulating system, surface treatment of the sample was not needed at all because the gas exchange was much faster than relaxation.

The described experiment demonstrates the feasibility of Fourier imaging under continuous flow of laser-polarized ^{129}Xe. This new technique will be useful for imaging studies of materials with short longitudinal relaxation time for ^{129}Xe.

VELOCITY IMAGING RESULTS

The pulse sequence used for imaging displacement probability profiles is shown in Fig. 1b. This modified pulsed gradient spin echo (PGSE) experiment shows a slice selection gradient in the same direction, namely the flow direction x, as the pulsed gradients (*13*). The displacement of the selected gas spins in flow direction during the fixed time Δ gives rise to a characteristic echo damping (*1, 14*). A second gradient (G_y) is applied to create the spatial resolution perpendicular to the flow direction. A 2D dataset $S(k, q)$ is acquired as a function of $k = (2\pi)^{-1}\gamma G_y t$ and $q = (2\pi)^{-1}\gamma \mathbf{g}\delta$. This type of combined *k*-space and *q*-space imaging is also known as dynamic NMR microscopy (*1, 14*). Fourier transformation with respect to q

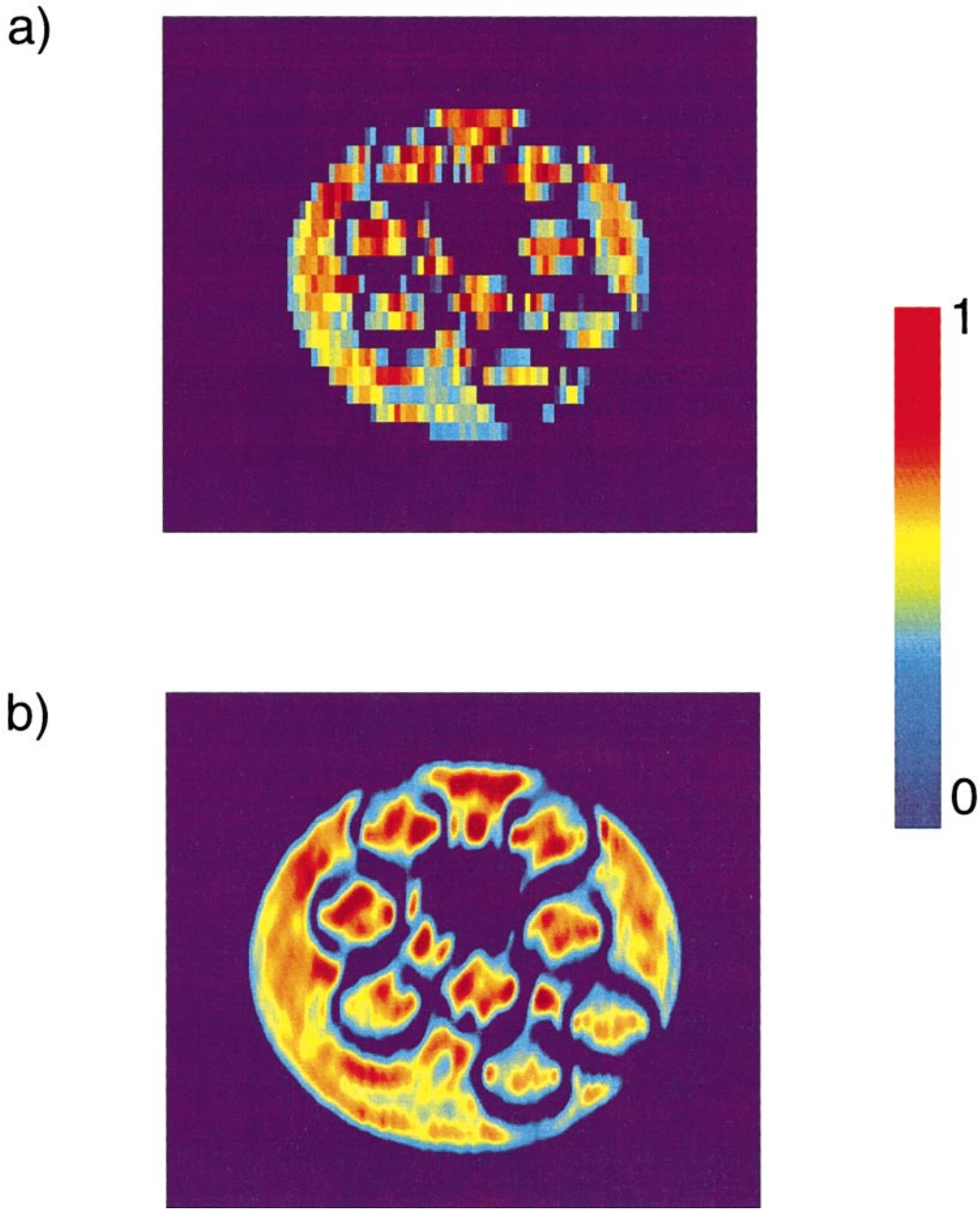

FIG. 2. Fourier image of laser-polarized ^{129}Xe flowing through a sample tube containing nine glass capillaries (wall thickness ~200 μm). A slice of 5 mm was selected. The upper image was obtained by 2D Fourier transform and a subsequent magnitude calculation of the raw data matrix (256 × 128) and shows the capillary walls as dark circles. The lower image was obtained by zero-filling to 512 × 512 points and interpolating using cubic splines. One capillary has sealed ends and remains dark (white dotted circle). A resolution of 120–150 μm is accessible at 0.4 MPa with our gradient setup that produces 0.6 T/m.

results in a displacement probability profile containing information about velocity and diffusion (*1*, *14*). The mean velocity is given by the position of the signal maximum. The width of the typically Gaussian profile is a function of the apparent diffusion coefficient and may include a velocity distribution.

Figure 3 shows the dynamic displacement profile of laser-polarized ^{129}Xe flowing through a glass tube (inner diameter = 6.3 mm) with a 3:1 constriction. The data were acquired as a 256 × 32 matrix (Δg = 0.018 T/m, Δ = 70 ms, δ = 150 μs, G_y = 0.15 T/m), followed by subsequent zero-filling to 256 × 256 points, and interpolated using cubic splines. The maximum velocity is observed in the center region of the tube (y = 0). The spin density in this region is low compared to that of other regions. This feature is due to the large velocity distribution in the center region (1–7 cm/s) and is not related to differences in longitudinal relaxation. In addition two negative velocity com-

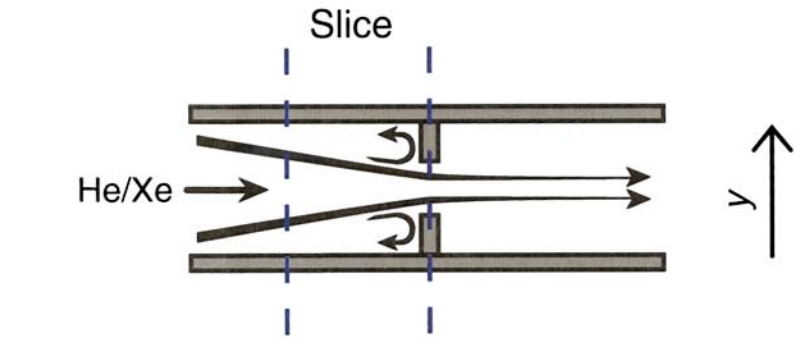

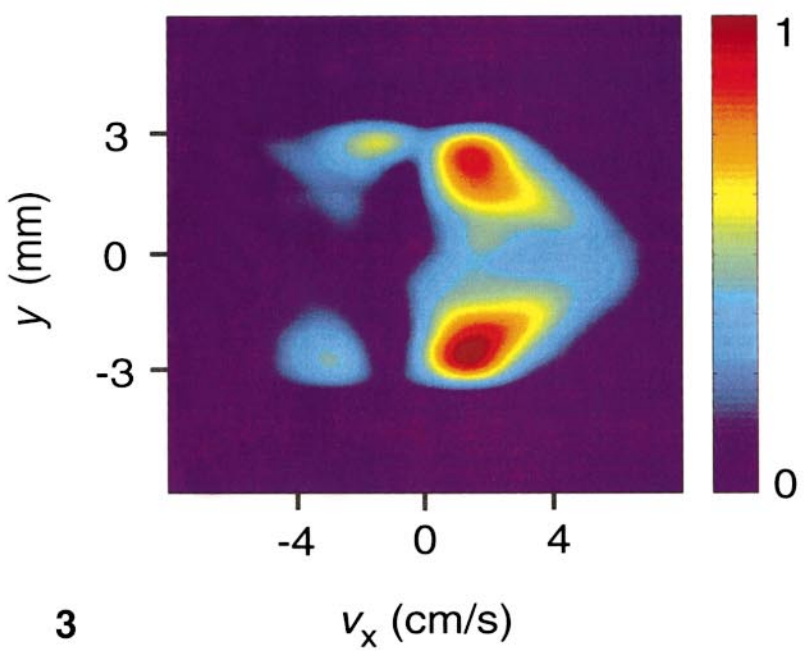

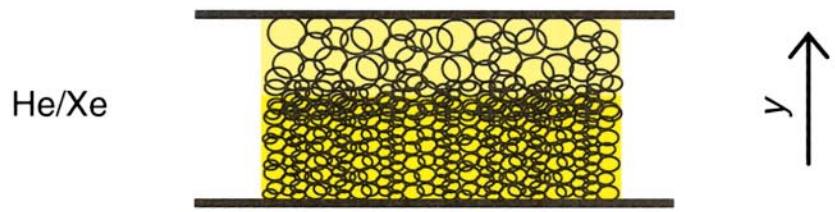

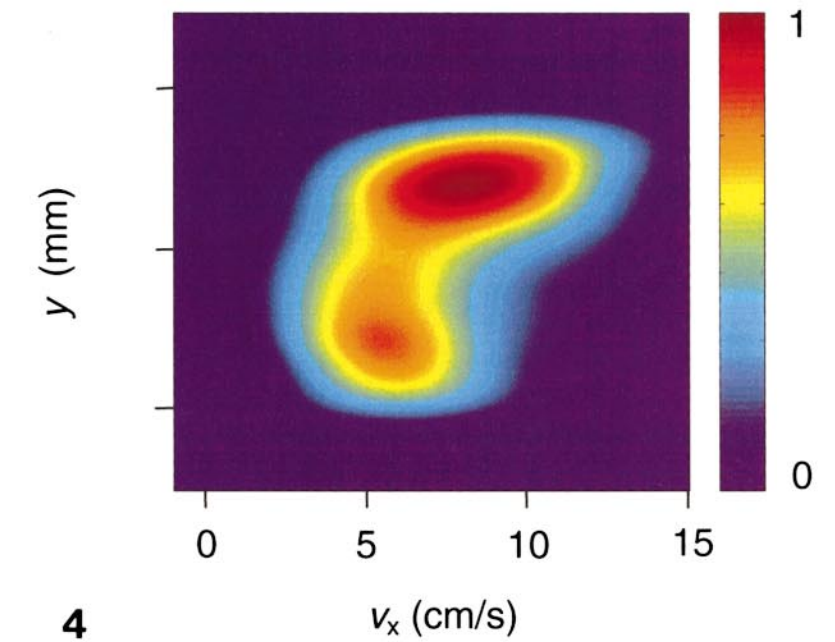

FIG. 3. Velocity profile in flow direction (x) of laser-polarized ^{129}Xe passing through a 3:1 constriction. A slice of 4 mm was selected upstream of the constriction. The image exhibits a back-flow upstream of the constriction identified by the negative velocity components. A broad distribution of velocities is visible in the center of the profile, starting at 1 cm/s and ending at 7 cm/s arising from acceleration (jet-flow) of the gas in the contraction region.

FIG. 4. Velocity profile of laser-polarized ^{129}Xe flowing through two different open-cell foams (PU). The lower permeability of the sample with higher density (bottom) is reflected in the slower velocity of 5.5 cm/s. A higher ^{129}Xe signal intensity is observed in the low-density PU foam. Slice thickness is 4 mm.

ponents are observed arising from back-flow close to the walls of the tube. This behavior may be explained by secondary flow vortices typical for laminar flow. The Reynolds number for the gas in the glass tube did not exceed 30. The viscosity used in this estimation was determined according to the equation given in Ref. (*15*) for multicomponent gas mixtures. The difference in the speed of the two components with negative velocity reveals that the contraction hole is not located in the center of the tube, a consequence of the glass-blowing process. The location of the back-flow was upstream of the constriction. This could be verified by velocity profiles, taken perpendicular to the flow direction.

Figure 4 shows a dynamic displacement profile of ^{129}Xe flowing through slices of two different polyurethane foams contained in a 3.5-mm id glass tube. The upper PU foam (low density) has a larger pore size (mean pore radius determined by optical microscopy: $\sim$200 μm), whereas the medium-density PU foam at the bottom has a smaller pore size (mean pore radius determined by optical microscopy: $\sim$100 μm). The mean gas velocity of 5.5 cm/s in the medium-density foam is lower compared to 8.1 cm/s observed for the low-density foam because the friction is higher.

In this paper we demonstrate a new technique that enhances the applicability of laser-polarized ^{129}Xe in MRI experiments. A variety of new applications of gas flow MRI are immediately obvious. From the fluid mechanics point of view, this new technique will be useful in studying gas flow under various conditions (e.g., laminar vs turbulent regimes). Another possible application of this technique is the study of diffusion and flow of gases in porous materials. Xenon is an inert gas and provides a nondestructive image contrast for a variety of porous media. Finally, the combination of MRI under continuous flow with polarization transfer (*16*) from laser-polarized ^{129}Xe to other spins (e.g., on solid surfaces) is possible and is being investigated in our laboratory.

ACKNOWLEDGMENTS

This work was supported by the Director, Office of Energy Research, Office of Basic Energy Sciences, Materials Sciences Division of the U.S. Department of Energy, under Contract DE-AC03-76SF00098. M.H. thanks the Studienstiftung des deutschen Volkes (Bonn, Germany) and the BASF AG for a postdoctoral fellowship. E.B. gratefully acknowledges a grant (Heisenberg-Stipendium) awarded by the Deutsche Forschungsgemeinschaft (Bonn, Germany). The authors thank Seth D. Bush for helpful discussions.

REFERENCES

1. P. T. Callaghan, "Principles of Nuclear Magnetic Resonance Microscopy," Oxford Univ. Press, London (1993).
2. M. J. Lizak , M. S. Conradi, and C. G. Fry, *J. Magn. Reson.* **95,** 548 (1991).
3. M. S. Albert, G. D. Cates, B. Driehuys, W. Happer, B. Saam, C. S. Springer, Jr., and A. Wishnia, *Nature* **370,** 199 (1994).
4. P. Bachert, L. R. Schad, M. Bock, M. V. Knopp, M. Ebert, T. Großmann, W. Heil, D. Hofmann, R. Surkau, and E. W. Otten, *Magn. Reson. Med.* **36,** 192 (1996).
5. Y.-Q. Song, H. C. Gaede, T. Pietrass, G. A. Barrall, G. C. Chingas, M.R. Ayers, and A. Pines, *J. Magn. Reson. A* **115,** 127 (1995).
6. D. M. Schmidt, J. S. George, S. I. Penttila, A. Caprihan, and E. Fukushima, *J. Magn. Reson.* **129,** 184 (1997).
7. M. Haake, A. Pines, J. A. Reimer, and R. Seydoux, *J. Am. Chem. Soc.* **119,** 11711 (1997).
8. B. Driehuys, G. D. Cates, E. Miron, K. Sauer, D. K. Walther, and W. Happer, *Appl. Phys. Lett.* **69,** 1668 (1996).
9. F. D. Doty, R. R. Inners, and P. D. Ellis, *J. Magn. Reson.* **43,** 399 (1981).
10. To avoid artifacts stemming from laser-polarized xenon outside the RF coil, it was necessary to run difference spectra. Every second scan was run without applying the Gaussian pulse and the resulting signal was sampled with negative receiver phase.
11. R. B. Bird, W. E. Stewart, and E. N. Lightfoot, "Transport Phenomena," Wiley, New York (1960).
12. T. M. de Swiet and P. N. Sen, *J. Chem. Phys.* **100,** 5597 (1994).
13. L. Frydman, J. S. Harwood, D. N. Garnier, and G. C. Chingas, *J. Magn. Reson. A* **101,** 240 (1993).
14. P. T. Callaghan and Y. Xia, *J. Magn. Reson.* **91,** 326 (1991).
15. I. F. Golubev, "Viscosity of Gases and Gas Mixtures," Translated from Russian, Israel Program for Scientific Translation, Jerusalem (1970).
16. G. Navon, Y.-Q. Song, T. Rõõm, S. Appelt, R. E. Taylor, and A. Pines, *Science* **271,** 1848 (1996).